

Molecular Docking and Dynamic Simulation of *Erythrina fusca* Lour Chemical Compounds Targeting VEGFR-2 Receptor for Anti-Liver Cancer Activity

Dila Aulia Maharani¹, Rosa Adelina^{1*}, Anggun Qurrota Aini², Supandi³

¹Pharmacy Department, Health Science Faculty, Syarif Hidayatullah Jakarta State Islamic University, Jl. Kertamukti, Cireundeu, South Tangerang, 15412, Indonesia

²Master of Forensic Science, Post Graduate School of Airlangga University, Jl. Airlangga 4-6, Surabaya, 60286, Indonesia

³Pharmaceutical Chemistry Department, Universitas Muhammadiyah Prof. Dr. Hamka, Jakarta, 13460, Indonesia

*Email: rosa.adelina@uinjkt.ac.id

Article Info

Received: Feb 13, 2024
Revised: Feb 23, 2024
Accepted: April 19, 2024
Online: June 09, 2024

Citation:

Maharani, D. A., Adelina, R., Aini, A. Q., & Supandi. (2024). Molecular Docking and Dynamic Simulation of *Erythrina fusca* Lour Chemical Compounds Targeting VEGFR-2 Receptor for Anti-Liver Cancer Activity. *Jurnal Kimia Valensi*, 10(1), 106 - 114.

Doi:

[10.15408/jkv.v10i1.35295](https://doi.org/10.15408/jkv.v10i1.35295)

Abstract

Liver cancer is a serious health concern characterized by abnormal cell growth, but currently, available treatment options are limited, suggesting the need for a new therapeutic method. Therefore, this research aimed to investigate the potential of chemical compounds obtained from the cangkring plant (*Erythrina fusca*) as anti-liver cancer agents targeting Vascular Endothelial Growth Factor Receptor 2 (VEGFR-2). The investigation was conducted in silico through molecular docking and dynamic method. Molecular docking was performed using AutoDock Tools, followed by visualization with Biovia Discovery Studio. Additionally, molecular dynamics simulation was conducted using GROMACS software and visualized with Grace. A total of 36 chemical compounds from *E. fusca* were used as ligands for molecular docking. The results showed that Isobavachalcone (ISB) was the most effective test compound with a binding energy of -11.45 kcal/mol, compared to the positive control Sorafenib with a value of -11.51 kcal/mol. In this context, hydrogen bonding, as well as hydrophobic, electrostatic, and unfavorable molecular interactions were identified. Moreover, molecular dynamics simulation provided RMSD, RMSF, Radius of Gyration (Rg), and hydrogen bond parameters. Analysis of these parameters further confirmed the superior stability of ISB in binding to VEGFR-2, suggesting the potential to suppress angiogenesis by blocking the receptor.

Keywords: *E. fusca*; VEGFR-2; Molecular Docking; Molecular Dynamic

1. INTRODUCTION

Liver cancer is an aggressive tumor often occurring in the context of chronic liver disease and cirrhosis¹. This was diagnosed among 905,677 people worldwide in 2020, with reports of 830,180 death cases². Vascular Epidermal Factor Receptor-2 (VEGFR-2), with the PDB code 4ASD, plays a crucial role in promoting angiogenesis by enhancing vascular permeability, endothelial cell survival, proliferation, migration or invasion of surrounding tissue, and capillary formation. VEGFR-2 pathway blocks tyrosine kinase activation³. Similarly, sorafenib approved by the Food & Drug Administration (FDA) for the systemic treatment of liver cancer functions as a multi-tyrosine kinase inhibitor⁴. This anti-angiogenic agent inhibits various growth factor

tyrosine kinase receptors such as VEGF, PDGF, and c-Kit, thereby blocking the Raf/MEK/ERK signal transduction pathway⁵. However, prolonged use of sorafenib can lead to drug resistance in cancer cells, suggesting the need for new treatment options. Many discoveries and developments of new anticancer agents are selective in inhibiting cancer cell proliferation pathways⁶.

Developing new drugs is costly and time-consuming, making computer-aided drug design (CADD) crucial for rapid production and expense reduction. CADD also known as an in silico method can efficiently identify various essential anticancer compounds⁷. In this context, molecular docking a structure-based in silico method, permits the virtual

screening of approved drugs, natural products, or compounds synthesized under a reasonable timeframe⁸. Molecular dynamics simulation can predict the stability of ligand-receptor complexes identified through molecular docking by producing suitable conformational states⁹. Previous research performing molecular docking and dynamics simulation on fourteen N-aryl methyl-aniline/chalcone hybrids synthesized against VEGFR-2 showed the inhibition of cancer cell growth¹⁰.

Erythrina fusca, commonly known as the cangkring plant, has potential for the treatment of liver cancer. Bioactivity exploration performed on *E. fusca* reported antibacterial, antimalarial, anti-estrogenic, estrogenic, anti-ischemic, reperfusion injury healing, and antiherpetic properties. Previous phytochemical screening of the aerial (above-ground) parts identified the presence of alkaloids, flavonoids, triterpenes, steroids, saponins, lactones, coumarins, reducing sugars, carotenoids, amines, and cardiac glycosides¹¹. Therefore, this research aimed to conduct a computational investigation of the interactions between chemical compounds from *E. fusca* Lour and VEGFR-2 receptor through molecular docking and dynamics simulation. The software used for this investigation included Pymol, AutoDock Tools, Biovia Discovery Studio, and Gromacs. Additionally, the objective was to identify chemical compounds from *E. fusca* with significant potential and suitable conformation for anti-liver cancer activity against VEGFR-2 using the in silico method, which has not been applied in previously published journals.

2. RESEARCH METHODS

The software used in this research was AutoDock Tools (<http://autodock.scripps.edu/>) for molecular docking simulation, PyMOL 2.5 by Schrödinger (<https://pymol.org>) for the preparation of ligands and macromolecule, MarvinSketch by ChemAxon (<https://chemaxon.com/products/marvin>) for ligand structure preparation, GROMACS (<https://www.gromacs.org/>) for molecular dynamics simulation, and Biovia Discovery Studio (<https://www.3ds.com/products-services/biovia/>) for visualization of molecular docking results. Other tools included Protein Data Bank (PDB) website (<https://www.rcsb.org/>) for downloading macromolecular structures, PubChem (<https://pubchem.ncbi.nlm.nih.gov/>) for downloading native and test ligands, CHARMM-GUI (<https://www.charmm-gui.org/>) for preparing materials applied in molecular dynamics, and Grace (<https://plasmagate.weizmann.ac.il/Grace/>) for visualization of molecular dynamic results.

Molecular docking was conducted on a laptop comprising 4 GB (Gigabyte) RAM (Random Access Memory), 11th Generation Intel(R) Core (TM) i3-1115G4 @ 3.00GHz 3.00 GHz Processor, Intel I3-

1115G4/ BGA CPU, 512G SSD, and Windows 11 (64bit). Meanwhile, molecular dynamics simulation was performed on a PC with specifications including Ubuntu 18.04.1 LTS, AMD Ryzen 7 2700x Eight-Core Processor x 16, GNOME 3.28.2, 64-bit, and 1 TB HDD connected to the internet. During these experiments, the materials used were the macromolecule VEGFR-2, the natural ligand sorafenib, and test ligands from chemical compounds of *E. fusca*.

Molecular Docking

Preparation of VEGFR-2 Macromolecule

VEGFR-2 macromolecule with the specific ID 4ASD was downloaded from the PDB website (<https://www.rcsb.org/>) in (*.pdb) format. This macromolecule was separated from the solvent (H₂O) and ligand using PyMOL, and then saved in (*.pdb) format. Subsequently, receptor optimization was performed through hydrogen and charge addition using AutoDock Tools, followed by saving the file in (*.pdbqt) format.

Preparation of native and test ligands

Ligands were downloaded from PubChem (<https://pubchem.ncbi.nlm.nih.gov/>), and then optimized by setting the *Torsion Tree* and adjusting the *number of active torsions* using *Autodock Tools*.

Lipinski analysis

Lipinski's rule of five (Ro5) analysis was performed on the site (<http://scfbio-iiitd.res.in/software/drugdesign/lipinski.jsp#anchortag>) by considering molecular weight ≤ 500 Da, hydrogen bond acceptor ≤ 10 , $\log P \leq 5$, and hydrogen bond donor ≤ 5 .

Docking Simulation

Redocking was performed with a natural ligand (sorafenib) after separation and optimization. In this context, the grid box was arranged as grid center $x = -24.964$, $y = -0.497$, and $z = -10.399$ with dimensions $40 \times 40 \times 40$ Å and spacing of 0.375 Å. Subsequently, the grid box configuration was saved in (*.gpf) format, and the grid process was executed using autogrid.exe binary software. The molecular docking stage included selecting receptors and ligands, followed by setting genetic algorithm parameters and configuring docking parameters. The docking document was saved with Lamarckian GA 4.2 in (*.dpf) format, and the docking process was run using autodock.exe.

Analysis and Visualization

Docking results in format (*.dlg) were analyzed using AutoDock Tools, focusing on binding energy (ΔG_{bind}) and inhibition constant (K_i). Furthermore, ligand and amino acid interactions were visualized, and the docked Ligand-Receptor Complex in (*.pdb) format

was opened with Biovia Discovery Studio 2019 for 2D and 3D visualization.

Molecular Dynamics

Receptor and Ligand Preparation

VEGFR-2 receptor and ligand were prepared for conduction of molecular dynamics simulation. Sorafenib and the best ligand obtained from docking analysis were used, then complexes formed between the protein and each ligand were saved in (*.pdb) format.

System Setup

Ligand-receptor complex format (*.pdb) files were input into CHARMM-GUI (<https://www.charmm-gui.org/>) using *Solution Builder on Input Generator*. During this process, topology generation, *water box creation*, ion addition, and *force field* selection were conducted.

System Minimization

System minimization was performed using the GROMACS application to prevent inappropriate collisions in the simulation system. Additionally, this helped loosen structural complexes by reducing potential energy to meet the requirements for simulation

Equilibration

Solvent and ions in the simulation system were equilibrated to achieve thermostat and barostat conditions at 310°K temperature and 1 atm pressure.

Production

The ligand-protein complex was subjected to molecular dynamics simulation to obtain an atomic trajectory.

Analysis of Molecular Dynamics Results

Production results were analyzed for parameters including RMSD, RMSF (Root Mean Square Fluctuation), Radius of Gyration (Rg), and hydrogen bonds, then atomic trajectories were visualized using Grace software.

3. RESULT AND DISCUSSION

The Lipinski Ro5 analysis was conducted to predict the physicochemical properties of the native and test ligands. Lipinski's Ro5 is a rule for designing drugs expected to penetrate membranes when administered orally. This includes molecular weight (BM) of no more than 500 g/mol, a partition coefficient (logP) value < 5, hydrogen bond donors < 5, and hydrogen bond acceptors < 10. Based on the rule, the positive control Sorafenib and 25 of the 36 test ligands met the four specified criteria.

In this context, physicochemical criteria for acceptable drug absorption and permeability constitute the first step in oral drug bioavailability¹².

The binding or active site of the receptor was determined¹³ using PyMOL by inputting the GDP file of the original ligand, followed by typing 'center of mass' on the PyMOL command line to obtain x, y, and z values (x = -24.964; y = -0.497; z = -10.399). Subsequently, the grid box was arranged as grid center x = -24.964, y = -0.497, and z = -10.399 with dimensions of 40x40x40 Å and spacing of 0.375 Å. This box was used as a reference for the molecular docking process of compounds to be tested. Additionally, the redocking results were analyzed with PyMOL, which produced an RMSD value of 1.136 Å, suggesting the applied docking procedure to be valid due to the generation of an RMSD < 2 Å. A greater RMSD value often leads to a larger deviation, while a smaller RMSD value makes the ligand pose resulting from docking to be closer to the crystallographic ligand pose.¹⁴

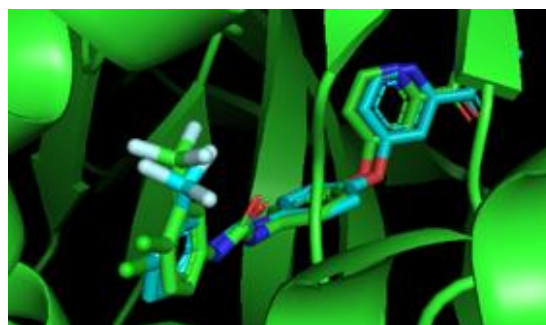


Figure 1. RMSD Result

Docking results stored in (*.dlg) format were analyzed using AutoDock Tools for parameters including binding energy and inhibition constants (Ki), then ligand and amino acid interactions were visualized. The binding energy value and Ki are parameters of the conformational stability of the investigated compounds in terms of affinity towards VEGFR-2 receptor¹⁵. The binding energy value was obtained through the interaction of the ligand with a receptor, which showed the suitability between the shape and size of the ligand and the binding site on receptor¹⁶. Moreover, molecular docking results of the native ligand Sorafenib showed a binding energy of -11.51 kcal/mol and a Ki value of 3.67 nM. The test ligand Isobavachalcone (ISB) had the smallest binding energy of -11.45 kcal/mol, which was close to the value obtained for Sorafenib, along with Ki of 4.05 nM. Negative binding energy leads to a lower Ki value due to a directly proportional relationship between both parameters¹⁷, as presented in the results shown in **Table 1**.

Table 1. Binding energy results and Ki against VEGFR-2 macromolecule

Ligand	Binding Energy (kcal/mol)	Inhibition Constant (Ki)
Sorafenib	-11.51	3.67 nM
Isobavachalcone	-11.45	4.05 nM
Vestitone	-8.94	281.56 nM
Erythraline	-8.92	290.19 nM
8-prenyldaidzein	-8.9	299.61 nM
Isoliquiritigenin	-8.87	317.46 nM
Erysodine	-8.83	336.63 nM
Lonchocarpol A	-8.7	417.45 nM
Wighteone	-8.65	459.55 nM
Liquiritigenin	-8.61	490.49 nM
Lupinifolin	-8.61	490.15 nM
Eryvarin D	-8.27	872.18 nM
Scandenone	-8.22	944.67 nM
Erysotrine <i>N</i> -oxide	-8.15	1.06 nM
Erythrisenegalone	-8.11	1.14 nM
Genistein	-8.07	1.22 nM
Demethylmedicarpin	-8.06	1.24 nM
Sandwicensin	-7.96	1.46 nM
Phaseollidin	-7.95	1.48 nM
3,7,4'-trihydroxyflavone	-7.88	1.68 nM
Citflavanone	-7.85	1.77 nM
Erytharbine	-7.84	1.79 nM
Erythribyssin A	-7.75	2.07 nM
Phaseolin	-7.72	2.19 nM
Erypoeigin I	-7.63	2.56 nM
Isovitexin	-7.42	3.63 nM
Phytol	-7.03	7.06 nM
Erythratidine	-6.89	8.86 nM
Hydroxycristacarpone	-6.85	9.56 nM
Orientanol A	-6.85	9.51 nM
Erythrabissyn I	-6.35	22.15 nM
Stigmasterol	-6.1	33.72 nM
Vitexin	-5.09	186.59 nM
β -amyrin	-4.59	4.89 nM
Lupeol	4.66	-
Schaftoside	18.39	-
Visenin-2	26.92	-

Interaction results visualized in 2D and 3D using Biovia Discovery Studio software are shown in **Figure 2**. These results presented the interactions of amino acid residues with ligands, showing potential contact between ligands and the protein that initiated inhibitory activity. The binding area or site is the point where ligands attach to a particular part of the protein, thereby influencing conformation and function. Additionally, the site shows amino acid residues forming interactions, such as hydrogen bonds, hydrophobic bonds, and electrostatic bonds, with the macromolecule and ligands ¹⁸. **Table 2** shows the interactions between the macromolecule and sorafenib, as well as the top 10 test ligands.

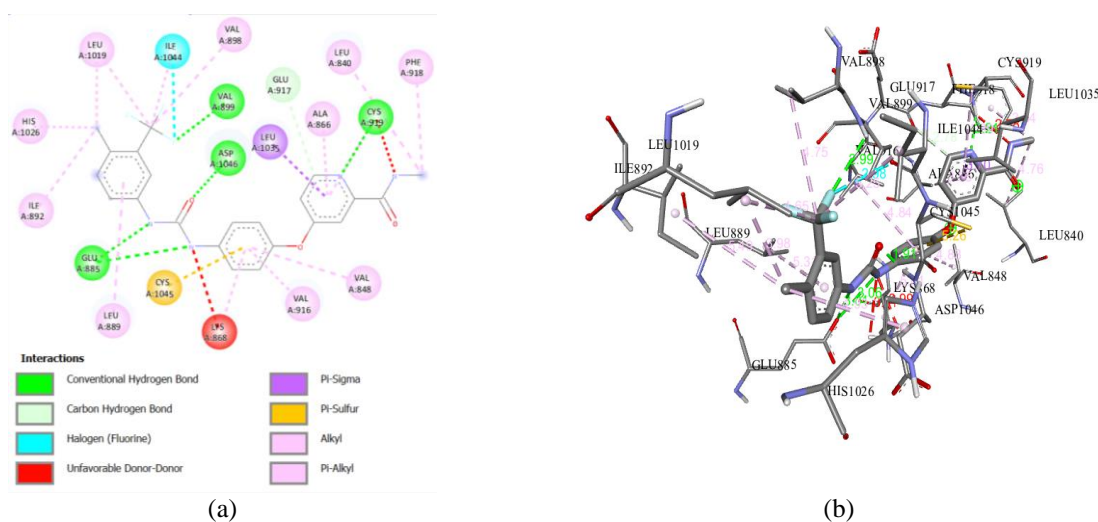
The native ligand Sorafenib as the positive control formed hydrogen bonds with VAL 899, CYS 919, ASP 1046, and GLU 885, as well as a carbon-hydrogen bond at GLU 917. The 31 test ligands formed

hydrogen bonds with amino acid residues partly identical to those bonded by the positive control. ISB also formed hydrogen bonds at residues CYS 919, ASP 1046, GLU 885, and GLU 917. Based on this perspective, more hydrogen bond formation increases the potential of ligand activity ¹⁹.

Sorafenib formed hydrophobic bonds with amino acid residue LEU 1035, which was similar to the interactions shown by the test ligand ISB. Moreover, ISB formed other identical hydrophobic bonds at residues ILE 892, LEU 1019, LEU 840, LEU 1019, ILE 1044, PHE 918, LEU 889, VAL 848, LYS 868, VAL 916, CYS 1045, ALA 866, and CYS 919. These hydrophobic bonds play an essential role in drug design due to the ability to enhance binding affinity between a drug and the target ²⁰.

Table 2. The results of VEGFR-2 macromolecule interactions with ligands

Ligand	Interaction Type	
	Hydrogen Bonds	Hydrophobic Interaction
Sorafenib (Positive Control)	VAL 899; CYS 919; ASP 1046; GLU 885; GLU 917	LEU 1035; ILE 892; LEU 1019; LEU 840; VAL 898; ILE 1044; PHE 918; HIS 1026; LEU 889; VAL 848; LYS 868; VAL 916; ALA 866; CYS 919
Isobavachalcone	CYS 919; ASP 1046; GLU 885; HIS 1026; GLU 917	LEU 1035; PHE 1047; ILE 892; LEU 1019; LEU 840; ILE 1044; PHE 918; LEU 889; VAL 848; LYS 868; VAL 916; CYS 1045; ALA 866; CYS 919
Vestitone	CYS 919; GLU 917; GLU 885	LYS 868; VAL 916; LEU 1035; LEU 840; PHE 918; LYS 868; VAL 899; LEU 840; VAL 848; ALA 866
Erythraline	LYS 868; GLY 893; VAL 899	LEU 889; ILE 892; VAL 898; VAL 899; LEU 1019; CYS 1045; HIS 1026
8-prenyldaizein	CYS 919; GLU 885	VAL 916; LEU 1035; LEU 889; VAL 899; VAL 848; ALA 866; CYS 1045; LYS 868; CYS 919
Isoliquiritigenin	CYS 919; VAL 914; ASP 1046	LYS 868; VAL 916; LEU 1035; LEU 840; ALA 866; CYS 919; VAL 848
Erysodine	LYS 868; GLU 885; VAL 899	LEU 889; ILE 892; VAL 898; LEU 1019; VAL 899; VAL 916; CYS 1045; HIS 1026
Lonchocarpol A	-	LEU 889; ILE 892; VAL 898; LEU 1019; ILE 888; CYS 1024; LYS 868; VAL 899; VAL 916
Wighteone	ASP 1046; GLU 885	LEU 889; VAL 916; VAL 848; LEU 840; LEU 1035; CYS 919; VAL 899; LYS 868; ALA 866; PHE 1047
Liquiritigenin	CYS 919; VAL 914; ASP 1046	LYS 868; VAL 916; LEU 1035; LEU 840; ALA 866; CYS 919; VAL 848
Lupinifolin	-	ILE 888; CYS 1024; CYS 817; LEU 889; LYS 868; VAL 899; VAL 916



(a) 2D visualization; (b) 3D Visualization of Sorafenib (Native Ligand)

were equilibrated for 125,000 steps and 125 picoseconds (ps) using the Parrinello-Rahman barostat method. Generally, this method maintains constant pressure and is recommended for NVT/NPT production simulation²⁶.

The molecular dynamics production stage was run for 5,000,000 steps and a time of 20 nanoseconds (ns). The production simulation of Sorafenib required 18 hours 46 minutes, while the duration for ISB was 18 hours 33 minutes. Simulation results were analyzed for parameters, including RMSD, RMSF, Rg, and hydrogen bonds, then atomic trajectories were visualized using xmgrace²⁷. These analyses determined the stability of the interactions between the ligands and receptors over space and time²⁸.

RMSD analysis determines the magnitude of binding pose changes over time, assessing the stability of ligand-protein interactions²¹. The graphical representation of RMSD values shows variations that occur during simulation²⁷. Initially, the backbone RMSD

simulation presented an increasing RMSD value, showing the protein structure opening and the process of ligand searching for suitable binding sites. Stabilizing RMSD values suggest the presence of interactions between protein residues and the ligand, which facilitates protein structure maintenance²⁹. The protein-BAX and protein-ISB complexes had RMSD values ranging from 0.175-0.225 nm, which were less than 3Å (0.3 nm), thereby suggesting good system (complex) stability³⁰. Meanwhile, RMSF analysis determines fluctuations in ligand interactions with amino acids during simulation. Bonded amino acid residues are presented in **Table 2** showing the results of VEGFR-2 macromolecule interactions with ligands²⁸. RMSF for binding residues ranged from 0.0394-0.0730 nm in the positive control complex and 0.0392-0.1026 nm in the ISB complex, with values less than 3Å (0.3 nm) suggesting good system (complex) stability³⁰.

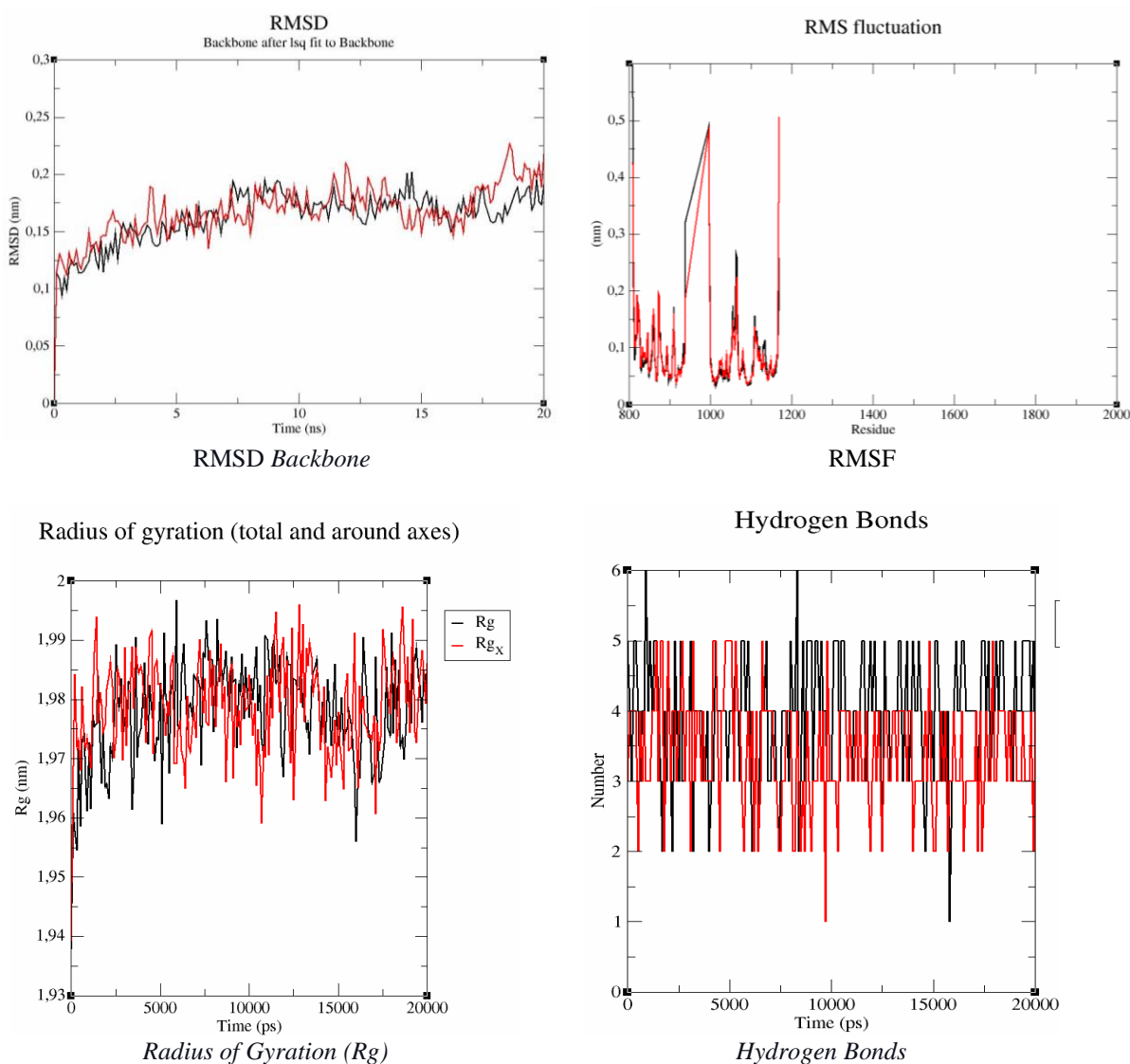


Figure 4. The Results of Molecular Dynamics Parameters (black = sorafenib; red = ISB).

The radius of Gyration (Rg) is defined as the distribution of protein atoms around the axis of a particular protein. When a ligand binds, a conformational change occurs, leading to alteration in Rg, which aids in predicting drug-protein compactness and binding patterns²⁷. During the 20000 ps simulation, Rg values ranged between 1.95-2.0 nm, with a graphical representation showing stable compactness for the two ligand-protein complexes formed in this research. Hydrogen bonds play an important role in the formation of receptor-ligand complexes³¹ and are often found among relatively stable compounds in molecular dynamics simulation³². From the results, it was observed that lower hydrogen bonding correlated with increased RMSD deviations²⁷. Meanwhile, the graph shows total hydrogen bonds formed during the 20,000 ps simulation, which presents stable interactions in both complexes.

4. CONCLUSION

In conclusion, molecular docking results of *E. fusca* chemical compounds showed that the best test ligand (ISB) had a binding energy of -11.45 kcal/mol, compared to the native ligand (Sorafenib) with a value of -11.51 kcal/mol. These chemical compounds interact with amino acid residues of the VEGFR-2 receptor through hydrogen, hydrophobic, and electrostatic bonds. Some of the residues that interacted with the investigated chemical compounds were similar to those bonded by the positive control. The amino acids included in the hydrogen bonds were CYS 919, ASP 1046, GLU 885, and GLU 917. Moreover, the stability of the ligand-protein bonds was confirmed through molecular dynamics simulation using ISB and Sorafenib. Molecular dynamics simulation produced RMSD, RMSF, Rg, and hydrogen bond parameters. ISB and Sorafenib complexes met the RMSD and RMSF value requirements of less than 3 Å (0.3 nm). Additionally, the Rg value was stable until the completion of the simulation, and the movements of the ligand-protein complexes were identical. The results of the hydrogen bond interactions between the two complexes were relatively stable per unit of time. Therefore, these hydrogen bonds played an essential role in receptor-ligand complexes formation.

REFERENCES

- Liu, C. Y., Chen, K. F. & Chen, P. J. Treatment of liver cancer. *Cold Spring Harb Perspect Med* 5, (2015).
- Rumgay, H. *et al.* Global burden of primary liver cancer in 2020 and predictions to 2040. *J Hepatol* 77, 1598–1606 (2022).
- Mutiah, R., Fawwaz Hariz, M., Yen, Y., Indrawijaya, A. & Ma'arif, B. In Silico Prediction of Isoliquiritigenin and Oxyresveratrol Compounds to BCL-2 dan VEGF-2 Receptors. *Indonesian Journal of Cancer Chemoprevention* (2019).
- Cervello, M. *et al.* Molecular mechanisms of sorafenib action in liver cancer cells. *Cell Cycle* 11, 2843–2855 (2012).
- Chen, C. & Wang, G. Mechanisms of hepatocellular carcinoma and challenges and opportunities for molecular targeted therapy. *World Journal of Hepatology* vol. 7 1964–1970 Preprint at <https://doi.org/10.4254/wjh.v7.i15.1964> (2015).
- Eweas, A. F., Khalifa, N. M., Ismail, N. S., Al-Omar, M. A. & Soliman, A. M. M. Synthesis, molecular docking of novel 1,8-naphthyridine derivatives and their cytotoxic activity against HepG2 cell lines. *Medicinal Chemistry Research* 23, 76–86 (2014).
- Nascimento, I. J. dos S., de Aquino, T. M. & da Silva-Júnior, E. F. The New Era of Drug Discovery: The Power of Computer-aided Drug Design (CADD) . *Lett Drug Des Discov* 19, 951–955 (2022).
- Pinzi, L. & Rastelli, G. Molecular docking: Shifting paradigms in drug discovery. *International Journal of Molecular Sciences* vol. 20 Preprint at <https://doi.org/10.3390/ijms20184331> (2019).
- Ferreira, L. G., Dos Santos, R. N., Oliva, G. & Andricopulo, A. D. Molecular docking and structure-based drug design strategies. *Molecules* vol. 20 13384–13421 Preprint at <https://doi.org/10.3390/molecules200713384> (2015).
- Hafeez, H. *et al.* Novel N-Arylmethyl-aniline/chalcone hybrids as potential VEGFR inhibitors: synthesis, biological evaluations, and molecular dynamic simulations. *J Enzyme Inhib Med Chem* 38, (2023).
- Anjum, A. *et al.* Flavonoid, pterocarpan and steroid from *Erythrina fusca* Lour. growing in Bangladesh: Isolation, and antimicrobial and free-radical scavenging activity. *Journal of Medicinal Plants* 20, 37–46 (2021).
- Chagas, C. M., Moss, S. & Alisaraie, L. Drug metabolites and their effects on the development of adverse reactions: Revisiting Lipinski's Rule of Five. *International Journal of Pharmaceutics* vol. 549 133–149 Preprint at <https://doi.org/10.1016/j.ijpharm.2018.07.046> (2018).
- Rachmania, R. A. S. and O. A. Larasati. Analisis In-Silico Senyawa Diterpenoid Lakton Herba Sambiloto (*Andrographis paniculata* Nees) pada Reseptor Alpha-Glucosidase sebagai Antidiabetes Tipe II. *Pharmacy: Jurnal Farmasi Indonesia (Pharmaceutical Journal of Indonesia)* 12, 210–222 (2015).
- Rena, S. R., Nurhidayah, N. & Rustan, R. Analisis Molecular Docking Senyawa Garcinia Mangostana L Sebagai Kandidat Anti SARS-CoV-2. *Jurnal Fisika Unand* 11, 82–88 (2022).
- Fakih, T. M., Jannati, F. A., Meilani, A., Ramadhan, D. S. F. & Darusman, F. Studi In Silico Aktivitas Analog Senyawa Zizyphine dari Bidara Arab (*Zizyphus spinachristi*) sebagai Antivirus SARS-CoV-2 terhadap Reseptor 3CLpro. *ALCHEMY Jurnal Penelitian Kimia* 18, 70 (2022).
- Kurnyawaty, N., Suwito, H. & Kusumattaqiin, F. Studi In Silico Potensi Aktivitas Farmakologi Senyawa Golongan Dihidrotetrazolopirimidin. *Jurnal Kimia* 172 (2021) doi:10.24843/jchem.2021.v15.i02.p07.

17. Cyntia Wibowo, M., Catherina Widjakusuma, E. & Ervina, M. Studi Pendahuluan Penambatan Molekul Senyawa Kandungan Dari Cinnamomi Cortex terhadap Epitop Respiratory Syncytial Virus (RSV). (2022).
18. Sari, I. W., Junaidin, J. & Pratiwi, D. Studi Molecular Docking Senyawa Flavonoid Herba Kumis Kucing (*Orthosiphon stamineus* B.) Pada Reseptor α -Glukosidase Sebagai Antidiabetes Tipe 2. *Jurnal Farmagazine* 7, 54 (2020).
19. Frimayanti, N. *et al.* Studi molecular docking senyawa 1,5-benzothiazepine sebagai inhibitor dengue DEN-2 NS2B/NS3 serine protease. *Chempublish Journal* 6, 54–62 (2021).
20. Varma, A. K. *et al.* Optimized hydrophobic interactions and hydrogen bonding at the target-ligand interface leads the pathways of Drug-Designing. *PLoS One* 5, (2010).
21. Lemkul, J. From Proteins to Perturbed Hamiltonians: A Suite of Tutorials for the GROMACS-2018 Molecular Simulation Package [Article v1.0]. *Living J Comput Mol Sci* 1, (2019).
22. Hassan, M. *et al.* Molecular docking and dynamic simulation of AZD3293 and solanezumab effects against BACE1 to treat alzheimer's disease. *Front Comput Neurosci* 12, (2018).
23. Lee, J. *et al.* CHARMM-GUI Input Generator for NAMD, GROMACS, AMBER, OpenMM, and CHARMM/OpenMM Simulations Using the CHARMM36 Additive Force Field. *J Chem Theory Comput* 12, 405–413 (2016).
24. Gerrard, J. A. & Domigan, L. J. *Protein Nanotechnology*. (Springer Science+Business Media, LLC, Auckland, New Zealand, 2020). doi:<https://doi.org/10.1007/978-1-4939-9869-2>.
25. Ali, A., Le, T. T. B., Striolo, A. & Cole, D. R. Salt Effects on the Structure and Dynamics of Interfacial Water on Calcite Probed by Equilibrium Molecular Dynamics Simulations. *Journal of Physical Chemistry C* 124, 24822–24836 (2020).
26. Ke, Q., Gong, X., Liao, S., Duan, C. & Li, L. Effects of thermostats/barostats on physical properties of liquids by molecular dynamics simulations. *J Mol Liq* 365, (2022).
27. Sneha, P. & Priya Doss, C. G. Molecular Dynamics: New Frontier in Personalized Medicine. in *Advances in Protein Chemistry and Structural Biology* vol. 102 181–224 (Academic Press Inc., 2016).
28. Zubair, M. S., Maulana, S. & Mukaddas, A. Penambatan Molekuler dan Simulasi Dinamika Molekuler Senyawa Dari Genus *Nigella* Terhadap Penghambatan Aktivitas Enzim Protease HIV-1. *Jurnal Farmasi Galenika (Galenika Journal of Pharmacy) (e-Journal)* 6, 132–140 (2020).
29. Zein Muttaqin, F., Ismail, H. & Nasrullah Muhammad, H. Studi Molecular Docking, Molecular Dynamic, Dan Prediksi Toksisitas Senyawa Turunan Alkaloid Naftiridin Sebagai Inhibitor Protein Kasein Kinase 2- α Pada Kanker Leukemia. *Pharmacoscrypt* 2, 49–64 (2019).
30. Supandi, Yeni & Dwita, L. P. Docking studies and molecular dynamics simulation of compounds contained in kaempferia galanga l. To lipoxygenase (lox) for anti-inflammatory drugs. *Journal of Mathematical and Fundamental Sciences* 53, 218–230 (2021).
31. Rashid, H. ur *et al.* Molecular docking and dynamic simulations of Cefixime, Etoposide and Nebrodenside A against the pathogenic proteins of SARS-CoV-2. *J Mol Struct* 1247, (2021).
32. Frimayanti, N., Dona, R. & Cahyana, F. Simulasi Molecular Dynamic (MD) Senyawa Analog Kalkon Sebagai Inhibitor Untuk Sel Kanker Paru A549. *Jurnal Penelitian Farmasi Indonesia* 9, (2020).